

Ellagic Acid-Changed Epigenome of Ribosomal Genes and Condensed RPA194-Positive Regions of Nucleoli in Tumour Cells

(ellagic acid / nucleolus / ribosomal genes / DNA damage)

S. LEGARTOVÁ¹, G. SBARDELLA², S. KOZUBEK¹, E. BÁRTOVÁ¹

¹Institute of Biophysics, Academy of Sciences of the Czech Republic, v. v. i., Brno, Czech Republic

²Epigenetic MedChem Lab, Università di Salerno Dipartimento di Farmacia, Fisciano, Salerno, Italy

Abstract. We studied the effect of ellagic acid (EA) on the morphology of nucleoli and on the pattern of major proteins of the nucleolus. After EA treatment of HeLa cells, we observed condensation of nucleoli as documented by the pattern of argyrophilic nucleolar organizer regions (AgNORs). EA also induced condensation of RPA194-positive nucleolar regions, but no morphological changes were observed in nucleolar compartments positive for UBF1/2 proteins or fibrillarin. Studied morphological changes induced by EA were compared with the morphology of control, non-treated cells and with pronounced condensation of all nucleolar domains caused by actinomycin D (ACT-D) treatment. Similarly as ACT-D, but in a lesser extent, EA induced an increased number of 53BP1-positive DNA lesions. However, the main marker of DNA lesions, γ H2AX, was not accumulated in body-like nuclear structures. An increased level of γ H2AX was found by immunofluorescence and Western blots only after EA treatment. Intriguingly, the levels of fibrillarin, UBF1/2 and

γ H2AX were increased at the promoters of ribosomal genes, while 53BP1 and CARM1 levels were decreased by EA treatment at these genomic regions. In the entire genome, EA reduced H3R17 dimethylation. Taken together, ellagic acid is capable of significantly changing the nucleolar morphology and protein levels inside the nucleolus.

Introduction

The nucleolus represents a highly organized compartment of the cell nucleus that is a prominent region of ribosomal gene transcription (Raška et al., 2004, 2006; Lam et al., 2005; Boisvert et al., 2007). The nucleolus is a dynamic, non-membrane-bound structure whose shape is maintained by acrocentric chromosomes carrying the ‘nucleolar organizer regions’ (NORs) (Chen et al., 2005; Olson and Dundr, 2005; Shav-Tal et al., 2005). The morphology of the nucleolus is tailored for ribosome biogenesis, and thus the nucleolus consists of three very important compartments responsible for production of pre-ribosomal particles, and subsequently mature 18S, 5.8S, and 28S rRNA (Raška et al., 2004, 2006; Lam et al., 2005; Boisvert et al., 2007). These compartments, well recognized by electron microscopy, are called the fibrillar centre (FC), the dense fibrillar component (DFC), and the granular component (GC) (e.g. Lam et al., 2005). An important breakthrough in the knowledge of biology of the cell nucleolus was brought by mass spectrometry showing the complex nucleolar proteome in isolated and purified nucleoli (Lam et al., 2005; Moore et al., 2011). Over 700 proteins of the nucleolus were identified by this technique (Scherl et al., 2002; Andersen et al., 2005). Such a huge amount of nucleolar proteins documents the complexity of the regulation of transcription of ribosomal genes. Alternatively, some of these proteins may be involved in DNA repair processes appearing in ribosomal genes. Generally, it is well known that transcription of ribosomal genes is mediated by RNA polymerase I, and this process likely occurs at the border between the FC and

Received December 16, 2014. Accepted January 22, 2015.

This work was supported by the Grant Agency of the Czech Republic projects P302/12/G157 and 13-07822S. Synthesis of the small molecular compound ellagic acid (EA) was supported by the Italian Ministry of Education, Universities, and Research (project PRIN 20103W4779).

Corresponding author: Eva Bártoová, Institute of Biophysics, Academy of Sciences of the Czech Republic, v. v. i., Královopolská 135, 612 65, Brno, Czech Republic. Phone: (+420) 541 517 141; Fax: (+420) 541240498; e-mail: bartova@ibp.cz (IBP ASCR)

Abbreviations: ACT-D – actinomycin D, AgNORs – argyrophilic nucleolar organizer regions, BSA – bovine serum albumin, ChIP – chromatin immunoprecipitation, DFC – dense fibrillar component, DMEM – Dulbecco’s Modified Eagle’s Medium, DMSO – dimethyl sulphoxide, EA – ellagic acid, FC – fibrillar centre, GC – granular component, GFP – green fluorescent protein, me2 – dimethylation, NBs – nuclear bodies, NORs – nucleolar organizer regions, PBS – phosphate-buffered saline, PCR – polymerase chain reaction, PI – propidium iodide.

DFC (Gonzalez Melendi et al., 2001; Raška, 2003). However, where exactly the transcription of ribosomal genes proceeds is still a matter of discussion, because some experiments showed that rDNA transcripts occur in the FC (e.g. Granboulan and Granboulan, 1965; Scheer and Benavente, 1990; Thiry et al., 2000). During rRNA processing, the pre-rRNA accumulates in the DFC, where posttranscriptional processing takes place. The compartment called GC is considered as a storage space for pre-ribosomal particles in various stages of maturation (Shaw and Jordan, 1995; Raška et al., 2006). Export of ribosomal subunits is mediated by simple diffusion, as has been described for 60S subunits (Politz et al., 2003). The nucleolus contains many regulatory proteins that also serve as detection targets by specific antibodies. For example, here we studied fibrillarin, RNA polymerase I subunit RPA194, or transcription factors UBF1 and UBF2 as markers of nucleoli. Similarly, nucleolin, interacting with different proteins and RNA sequences, is highly abundant in the nucleolus. The above-mentioned proteins have a major regulatory role in ribosome particle biogenesis and some of them are responsible for maintenance of nucleolar chromatin structure, and thus regulate chromatin condensation/de-condensation in the nucleolus (Erard et al., 1988).

The nucleolus is also highly sensitive to genome injury, and thus represents a central nuclear compartment with pronounced ability for the stress response. For example, nucleolar functions play a role during stress-induced regulation of tumour suppressor p53, which is mutated in the majority of cancer cells (Boulon et al., 2010). Cellular stress also induces changes in the organization and compactness of the nucleolus, which can appear after genome irradiation or cytostatic treatment. Moreover, widely used transcription inhibitor actinomycin D (ACT-D), inhibiting RNA polymerase I, also has the ability to induce DNA lesions (Govoni et al., 1994; Al-Baker et al., 2005). ACT-D treatment leads to segregation of the nucleolus characterized by condensation of nucleolar regions, and subsequently the FC and GC are separated (Shav-Tal et al., 2005). Different types of caps (central nucleolar bodies) are formed by nucleolar proteins such as UBF1/2 or coilin when cells are treated with ACT-D. Based on these results it seems to be important to study the effects of potential cytotoxic drugs, including ACT-D, on the nucleolus compartments. This is important especially in tumour cells, characterized by an increase in the number of nucleoli. Also, studies of the nuclear pattern of argyrophilic nucleolar organizer regions (AgNORs) after tested treatments may be valuable in tumour cells, because aberrant morphology of AgNORs was well described in malignancies and this morphological parameter can serve as a diagnostic tool (Derenzini, 2000).

These results inspired us to study the effect of ellagic acid (EA), which was identified in pomegranate and other fruit extracts. EA represents an inhibitor of arginine methyltransferase CARM1 (Kim et al., 2004; Selvi et al., 2010). We therefore tested EA as a natural prod-

uct, an ‘epi-drug’, which affects the epigenome of mammalian cells. EA is also characterized by its anti-proliferative effect (Kim et al., 2004; Selvi et al., 2010). Here, we studied whether EA is capable of changing the nucleolar morphology and the pattern of selected proteins of the nucleolus as very important targets of anti-cancer therapy.

Material and Methods

Cell cultivation and counting

Human cervical adenocarcinoma HeLa cells and HeLa cells expressing GFP-tagged histone H2B (generous gift from Dr. Marion Cremer, Ludwig-Maximilian-University of Munich, Germany) were cultivated in Dulbecco’s Modified Eagle’s Medium (DMEM, Sigma-Aldrich, Prague, Czech Republic), supplemented with penicillin and streptomycin, and 10% foetal bovine serum (PAN Biotech GmbH, Aidenbach, Germany). Cells were maintained on Petri dishes at 37 °C, 5% CO₂ in a humidified thermostat. For the experiments, cells were harvested at approximately 70–80 % confluence. At this confluence we treated the cells (24 h after seeding) with CARM1 inhibitor (EA; Selvi et al., 2010) and ACT-D (Horáková et al., 2010). EA binds to the XXPRX/XXRPX motif on histone H3, but does not directly bind to the catalytic domain of CARM1 (Kim et al., 2004). Intriguingly, H3R26 methylation, which is also mediated by CARM1, should not be inhibited by EA because it does not contain the proline-arginine motif (Selvi et al., 2010). We used the following concentration of EA: 250 µM for 24 h. For comparison we tested the effect of 0.5 µg/ml actinomycin D [#A9415, Sigma-Aldrich, treatment for 2 h]. The drugs were diluted in dimethyl sulphoxide (0.05% DMSO). EA concentration was established according to the cell proliferation rate measured as the cell numbers in control non-treated cells and after the cell treatment. Cell counting was performed by automatic cell counter TC-10 (BIO-RAD, Prague, Czech Republic). Concentration of ACT-D was also optimized according to our former experimental approaches (Horáková et al., 2010; Stixová et al., 2011, 2012).

Analysis of the cell cycle by flow cytometry

For flow cytometric analyses, the cells were washed twice in PBS, fixed for 30 min in ice-cold 70% ethanol, and stored at 4°C before measurement. Fixed cells were washed in phosphate-buffered saline (PBS) and stained with FxCycle™ PI/RNase Staining Solution [#F10797, Invitrogen™, Life Technologies, Prague, Czech Republic] for 30 min at 37 °C. The DNA content was determined according to the fluorescence of incorporated propidium iodide (PI) by flow cytometer BD FACS Canto II (488-nm argon laser for excitation, Becton-Dickinson, Czechia, s.r.o., Prague, Czech Republic). Distribution of the cells in individual cell cycle phases was measured and analysed using the BD FACS Diva

software (Becton-Dickinson) and FlowJo software (Tree Star, Ashland, OR); (<http://www.flowjo.com>). Three independent repetitions consisting of triplicates were analysed for control samples and cells treated with EA or ACT-D.

AgNOR staining

Cells were treated for 15 min with 75 mM KCl at 37 °C, fixed with methanol/acetic acid mix (3 : 1), and placed at -20 °C for 30 min. Cell nuclei were spread on microscope slides and dehydrated in 70%, 80%, and 96% ethanol (cooled at -20 °C) for 1 min each. Nuclei were stained for 30 min in the dark, and the following mixtures were used for staining: mixture A (2% gelatin dissolved in double-distilled water [ddH₂O] and 1% formic acid) and mixture B (50% AgNO₃ dissolved in ddH₂O). Mixtures A and B were diluted at a 1 : 2 ratio. Nuclei were stained for 15 min using Eosin Y solution (Sigma-Aldrich; #HT110180). Specimens were dehydrated for 1 min in 96%, 80%, and 70% ethanol at room temperature. Cells were mounted in Vectashield mounting medium (Vector Laboratories, Burlingame, CA; #H-1000) and analysed using a transmission light mode by a Leica SP5 X confocal microscope (Leica Microsystems, Mannheim, Germany, represented by Micro, s.r.o., Brno, Czech Republic).

Immunofluorescence analyses, cell visualization by confocal microscopy, quantification of fluorescence intensity

Cells were washed in PBS and fixed for 10 min in 4% formaldehyde. Cells were permeabilized with 0.1% Triton-X (8 min) and 0.1% saponin (12 min). Then the cells were washed in PBS and blocked for 1 h using 1% bovine serum albumin (BSA) in PBS. Incubation with the primary antibodies was performed overnight in the dark at 4 °C. Antibodies were diluted in 1% BSA; dilution was 1 : 100–1 : 200. The cells were then washed in PBS and incubated with secondary antibody. DNA was stained using 4',6-diamidino-2-phenylindole (DAPI). The primary antibodies were as follows: anti-fibrillarin (#ab5821, Abcam, Cambridge, UK), anti-UBF1/2 (#sc9131; Santa Cruz Biotechnology, Inc., Heidelberg, Germany); anti-RPA194 (#sc48385; Santa Cruz Biotechnology, Inc.); anti-53BP1 (#ab21083; Abcam); anti-γH2AX (#ab2893; Abcam). For fluorescence staining we used secondary antibody Alexa Fluor® 594 Donkey Anti-Rabbit IgG (H+L) (#A-21207, Invitrogen™, Life Technologies).

Cells stained by immunofluorescence were inspected and representative images acquired using confocal microscopy Leica DMRXA, equipped by rotating Nipkow discs, objective 100x, numerical aperture (NA = 1.4.) (Leica Microsystems). Images were converted to TIFF format and quantification of fluorescence intensities was performed by NIH ImageJ software (freeware) according to selected lines crossing the nucleoli, and histograms were created.

Chromatin immunoprecipitation assays and polymerase chain reaction (ChIP-PCR)

ChIP procedures were performed according to the manufacturer's protocol (#17-295, ChIP Assay Kit, Merck-Millipore, Prague, Czech Republic) and as we described elsewhere (Strašák et al., 2009; Foltánková et al., 2013). For ChIP we used the following antibodies (5 µl each): anti-fibrillarin (#ab5821, Abcam), anti-UBF1/2 (#ab75781; Abcam); anti-53BP1 (#ab21083; Abcam); anti-γH2AX (#ab2893; Abcam), and anti-PRMT4 (syn. CARM1; #ab128851; Abcam). As negative controls, we used samples precipitated without antibody and samples immunoprecipitated with anti-rabbit IgG (#A-4914, IgG whole molecule, Sigma-Aldrich). Immunoprecipitation reactions were performed overnight at 4 °C. Histone-DNA immuno-complexes were incubated for 2 h at 4 °C with protein A agarose beads and washed with appropriate buffers as recommended by the manufacturer (#17-295, buffers were purchased from Merck-Millipore). Elution was performed in 0.1 M NaHCO₃ with 1% SDS. Histone-DNA crosslinks were released by incubation for 6 h at 65 °C. ChIP-DNA was isolated using the QIAamp® DNA Mini kit (#51304, QIAGEN, represented by Dynex Technologies, s. r. o., Buštěhrad, Czech Republic) and purified DNA was used for PCR. Primers used to detect ribosomal genes have been previously described (Horáková et al., 2010).

Western blot analyses

Western blot analyses were performed according to Stixová et al. (2012). For analyses, we used the following primary antibodies: anti-fibrillarin (#ab5821, Abcam); anti-UBF1/2 (#ab75780, Abcam); anti-53BP1 (#ab21083; Abcam); anti-γH2AX (#ab2893; Abcam), anti-PRMT4 (syn. CARM1; #ab128851; Abcam), anti-H3R17me2 (#ab8284, Abcam); anti-α-tubulin (#LFPA0146, Fisher-Scientific, Waltham, MA). Total protein levels were measured by µQuant spectrophotometer (BioTek, represented by Dynex Technologies, s.r.o., Buštěhrad, Czech Republic) and the density of Western blot fragments was normalized to the total protein levels and finally to the level of α-tubulin. Quantification of the fragment density was performed by NIH ImageJ software.

Statistical analysis

For statistical analysis we used Student's *t*-tests, calculated by the SigmaPlot software (version 13.0; Jandel Scientific, San Jose, CA). As statistically significant differences between parameters measured in control and treated cells we considered values at $P \leq 0.05$. For ChIP-PCR quantification, significantly increased values for EA (ACT-D) from control samples are marked by * (#). Decreased values are pointed out by red signs * (#). Significantly different values from control samples, shown for other experiments, are labelled by asterisks (*). Statistical significance for Student's *t*-tests was additionally compared with the relevant table in Rohlf and Sokal (1995).

Results

The effect of ellagic acid reduced cell proliferation and blocked the cells in G2-M phase of the cell cycle

As the first step, we tested the effect of EA, known as a CARM1 inhibitor (Selvi et al., 2010; Castellano et al., 2012), on HeLa-GFP-H2B cell numbers. Doses of 200 μ M and 250 μ M significantly reduced the cell numbers to 70–80 % of control values (Fig. 1A). For all experiments we used 250 μ M EA inhibitor in order to potentially affect morphology and epigenetic profiles of the nucleoli. As a control agent changing the morphology of nucleoli and affecting transcription of ribosomal genes we used actinomycin D (ACT-D). As an additional parameter showing the cell proliferation rate (analysis of S phase), we studied the cell cycle profile by flow cytometry. Both EA and ACT-D caused cell cycle arrest in G2-M phase of the cell cycle and reduced S phase (Fig. 1B). Especially after EA treatment, mitotic cells

were well visible by fluorescence microscopy (visual observation).

Ellagic acid changed the morphology of AgNORs, nucleolar proteins RPA194, UBF and fibrillarin

We tested the effect of EA on the morphology of nucleoli. For such analyses the cells were stained by silver (Ag) in order to visualize NORs. We studied these regions in standard HeLa cells and HeLa cells stably expressing GFP-tagged histone H2B (Fig. 2A, B). We found that EA has the ability to change the morphology of AgNORs in HeLa tumour cells. In contrast to crescent-like morphology of AgNORs after ACT-D treatment, EA induced highly compact, large, and silver-dense nucleoli in HeLa cells (Fig. 2A, B).

Based on these changes in AgNOR morphology, we additionally analysed the pattern of selected nucleolar proteins, including RPA194, UBF1/2, and fibrillarin (Fig. 3A, B and Fig. 4). ACT-D caused a 100% effect leading to formation of compact RPA194-, UBF1/2-po-

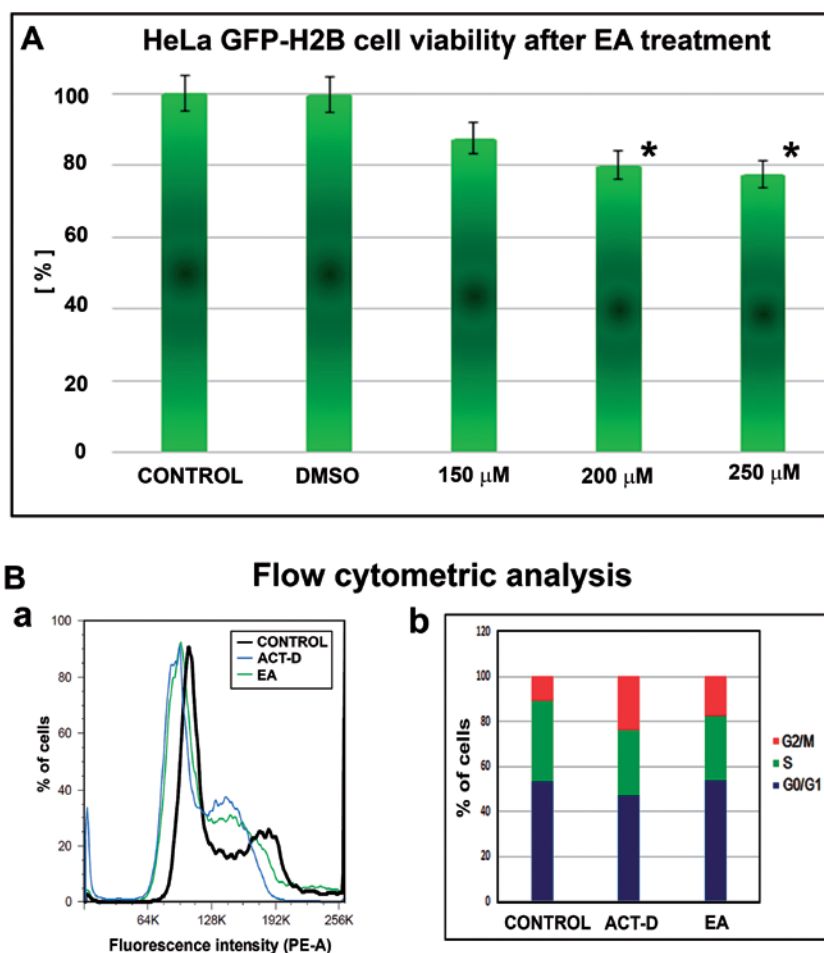


Fig. 1. Cell proliferation parameters affected by ellagic acid and actinomycin D in HeLa-GFP-H2B cells. **(A)** Cell numbers after the treatment with 150 μ M, 200 μ M and 250 μ M of EA in comparison with non-treated control cells and cells affected by DMSO, used for EA dilution. Percentage of the cells \pm standard errors are shown. Asterisks (*) indicate significantly different results from control values shown as 100 %. **(B)** Results of cell cycle analyses measured by flow cytometry according to fluorescence intensity of incorporated propidium iodide. The number of cells in individual cell cycle phases (G1, S and G2-M) was analysed (see histogram and summarizing bar chart).

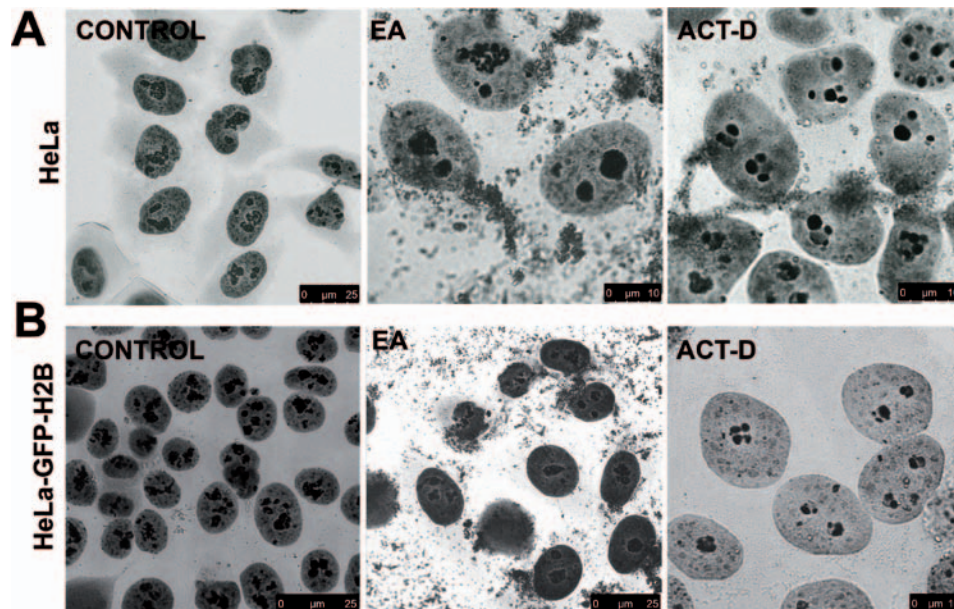


Fig. 2. Morphology of argyrophilic nucleolar organizer regions. AgNORs (black) were studied in (A) standard HeLa cells and (B) HeLa cell stably expressing GFP-H2B. AgNORs were visualized in control non-treated cells and cells exposed to EA and ACT-D. Transmitted light was used for visualization and AgNORs were recognized as black regions inside the cell nuclei (grey). Analysis was performed by wide-field microscopy.

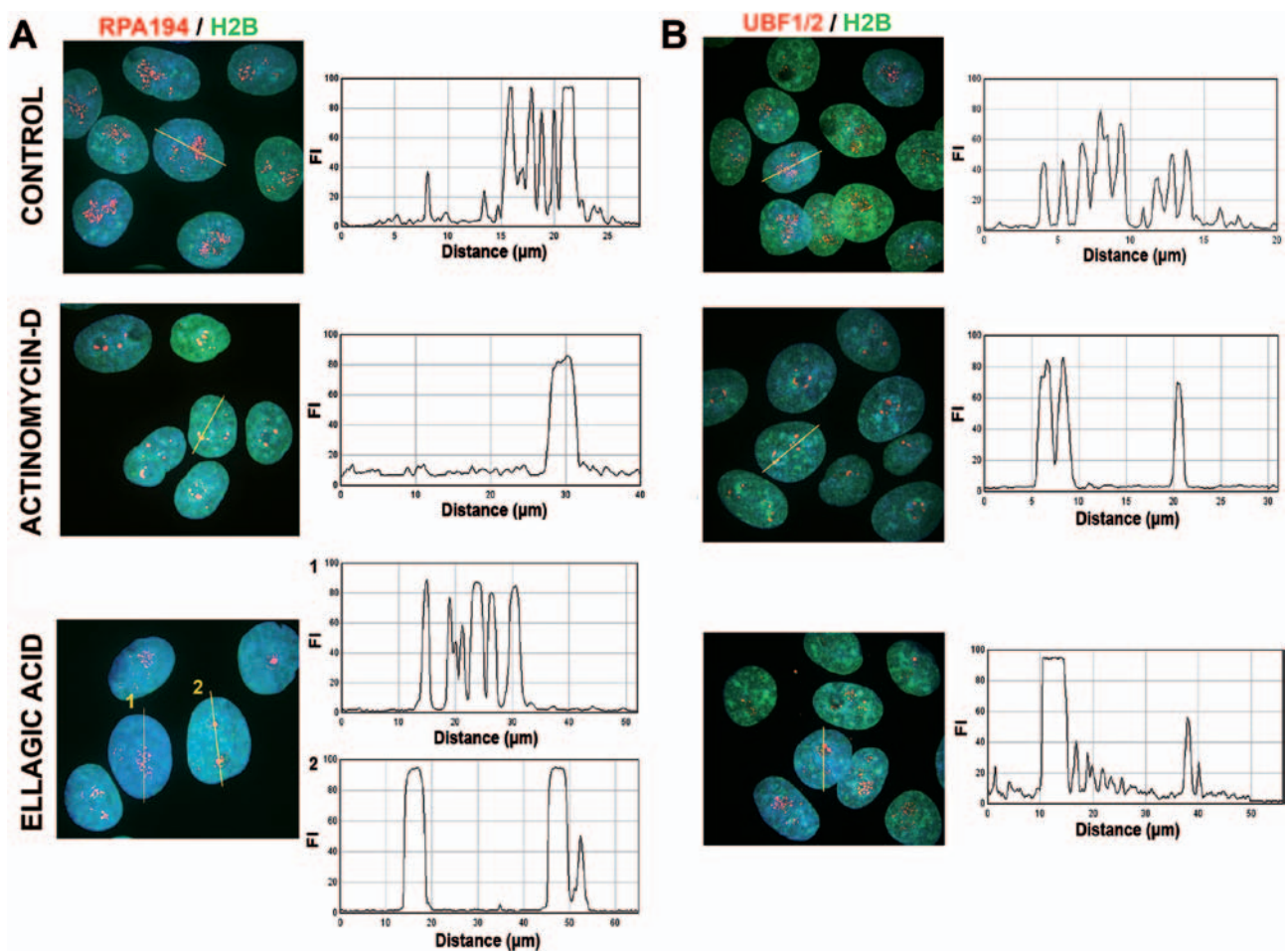


Fig. 3. Nuclear pattern of RPA194 and UBF1/2 in cells treated with EA and ACT-D. (A) RPA194 and (B) UBF1/2 accumulation patterns (red) were studied in HeLa cells stably expressing GFP-tagged histone H2B (green). Quantification of fluorescence intensities was performed by ImageJ software according to selected lines crossing the nucleoli and histograms were created.

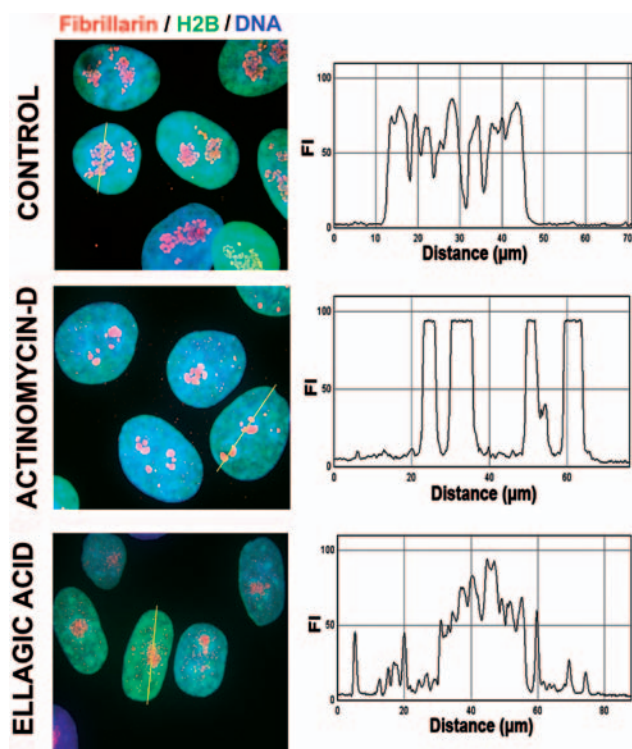


Fig. 4. Nuclear pattern of fibrillarin in cells treated with EA and ACT-D. The fibrillarin accumulation pattern (red) was studied in HeLa cells stably expressing GFP-tagged histone H2B (green). Quantification of fluorescence intensities was performed by ImageJ software according to selected lines intersecting the nucleoli and related histograms are shown.

sitive and fibrillarin-positive regions of the nucleoli (Figs. 3, 4). However, EA induced similar morphology of the studied proteins as ACT-D in only RPA194-positive regions (Fig. 3A). Approximately 50 % of the cells were characterized by EA-induced morphological changes of RPA194 protein (Fig. 3A). The rest of the cells were characterized by an identical pattern of RPA194-positive regions as observed in control, non-treated cells (see especially quantification in Fig. 3A). In the case of UBF1/2- and fibrillarin-positive regions, EA did not significantly influence the pattern of these proteins, which was nearly identical to control, non-treated cells. Only ACT-D caused the expected condensation of UBF1/2- and fibrillarin-positive regions of the nucleoli (Figs. 3 and 4).

Ellagic acid increased the number of 53BP1- and γ H2AX-positive DNA lesions

We also tested whether ACT-D and EA induce genome injury. For these analyses we selected 53BP1 and γ H2AX as markers of DNA damage (Fig. 5A-C). By immunofluorescence and confocal microscopy, we observed an increased number of 53BP1-positive foci after ACT-D treatment and in a lesser extent after EA treatment (Fig. 5C, D). EA-treated cells were characterized in approximately 60 % by a pattern of 53BP1 NBs simi-

lar to control cells and in 40 % there was a pattern of 53BP1 NBs specific for ACT-D treatment (Fig 5C, E). Conversely, γ H2AX was not accumulated into compact foci after ACT-D and EA treatment, but an increased level of γ H2AX in the entire genome was found according to fluorescence intensity in both ACT-D- and EA-treated cells (Fig. 5B).

Ellagic acid increased the level of fibrillarin, UBF1/2, γ H2AX, and decreased the level of 53BP1 and CARM1 at the promoter regions of ribosomal genes

Because of the effects of EA and ACT-D on the morphology of the nucleolus, we tested the abundance of fibrillarin, UBF1/2, 53BP1, γ H2AX and CARM1 at the promoters of ribosomal genes and genomic regions encoding 28S rRNA. Using CHIP-PCR we observed EA-induced increase in the level of fibrillarin, UBF1/2, and γ H2AX, while EA reduced the level of 53BP1 and CARM1 at the promoter regions of ribosomal genes (Fig. 6A, B). The region encoding 28S rRNA was characterized by only an increase in γ H2AX after EA treatment (Fig. 6A, B). ACT-D caused an increase in fibrillarin, γ H2AX and CARM1 at the promoters of ribosomal genes, while 53BP1 was decreased after this treatment (Fig. 6A, B). In the region encoding 28S rRNA we observed that ACT-D increased the level of CARM1 (Fig. 6A, B).

Global levels of fibrillarin, UBF1/2, 53BP1 and CARM1 in the entire genome were not changed, but H3R17me2 was reduced and γ H2AX increased by ellagic acid

Additionally, we tested the effects of ACT-D and EA on the protein level in the entire cell nucleus (Fig. 7A). By Western blots we found that both ACT-D and EA did not change the global levels of fibrillarin, 53BP1, and CARM1 when normalized to α -tubulin. The level of UBF1/2 was increased by ACT-D treatment (Fig. 7A, B). The level of γ H2AX was increased only by stimulation of the cells with EA (Fig. 7A). The entire level of H3R17me2 was significantly reduced by EA treatment of HeLaGFP-H2B cells when normalized to α -tubulin (Fig. 7B).

Discussion

Nucleolus consists of many proteins, including upstream binding factors UBF1/2, polymerase I, nucleolin, nucleophosmin or fibrillarin. These proteins of immense functional roles are anchored in individual compartments of the nucleolus (FC, DFC or GC) and they can relocate upon genome injury. Numerous factors displaying effects on the morphology of nucleoli have been described, e.g., various sources of radiation, infection by viruses, or cell treatment with cytotoxic agents, including tested inhibitor of RNA polymerase I,

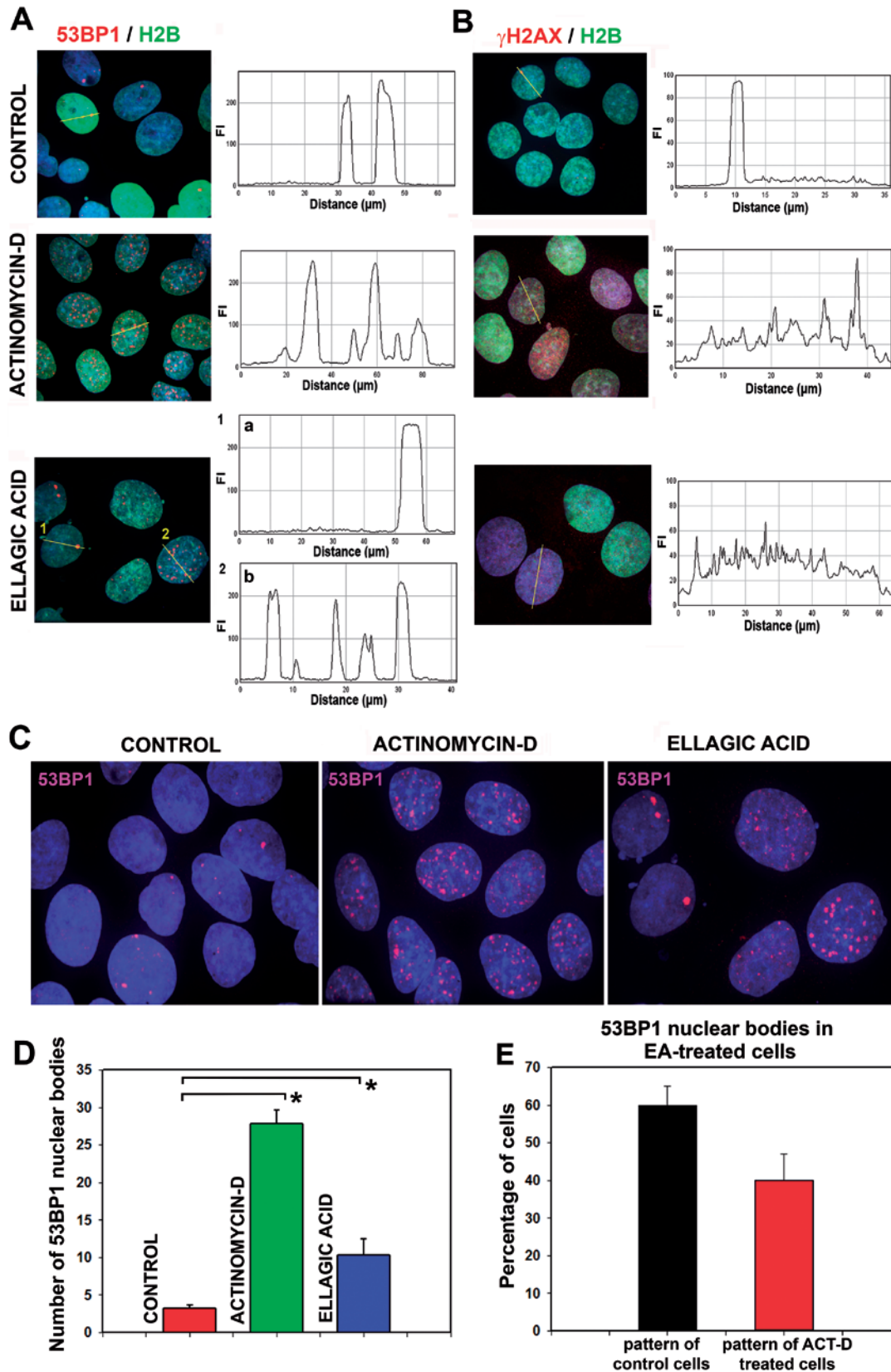


Fig. 5. Nuclear pattern of 53BP1 and γ H2AX in cells treated with EA and ACT-D. (A) 53BP1 and (B) γ H2AX nuclear distribution patterns (red) were studied in HeLa cells stably expressing GFP-tagged histone H2B (green). Quantification of fluorescence intensities by ImageJ software was done according to selected lines crossing the nucleoli and histograms are shown. (C) The number of 53BP1-positive DNA damage-related nuclear bodies (pink) was analysed in standard HeLa cells [cell nuclei were stained with DAPI (blue)], treated with EA and ACT-D. Quantification of the number of 53BP1 nuclear bodies is shown in panel (D). Panel (E) shows the percentage of EA-treated cells with the pattern of 53BP1 nuclear bodies similarly as in control cells (black bar) or in ACT-D-treated cells (red bar).

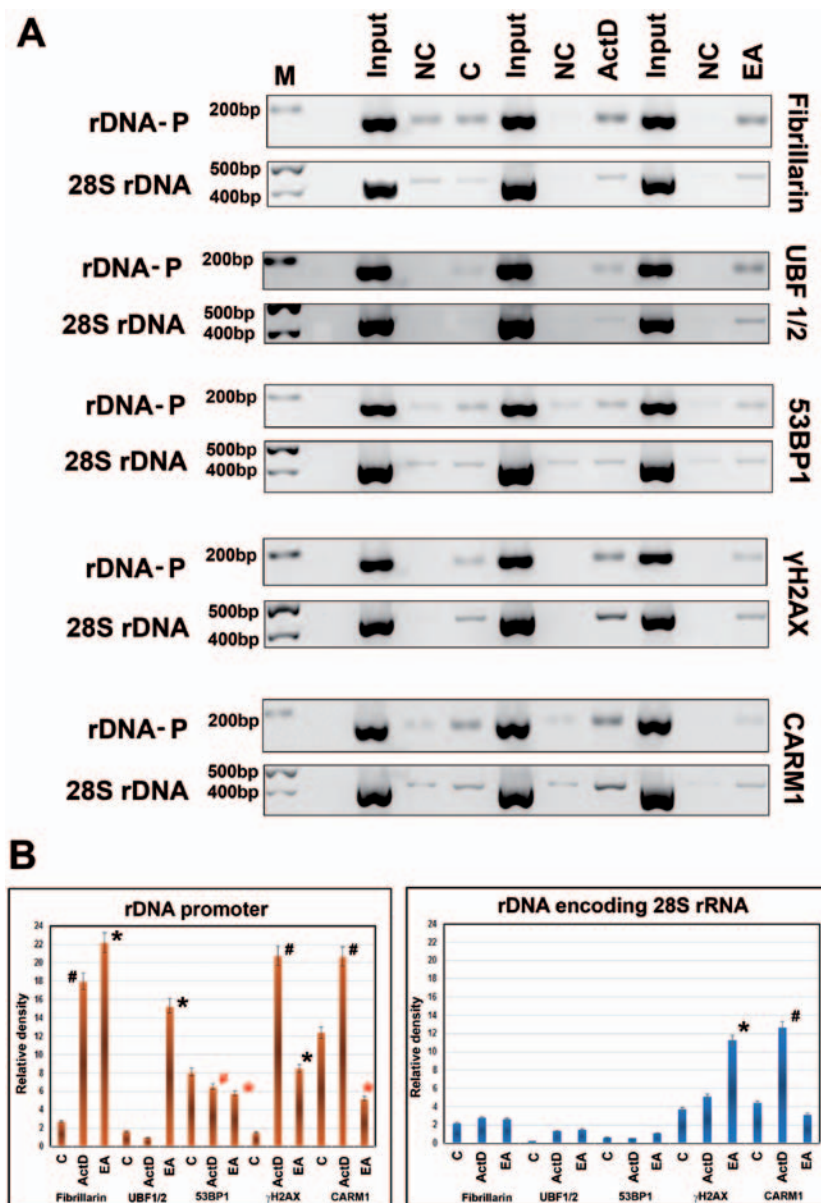


Fig. 6. ChIP-PCR analysis of ribosomal genes after the treatment with EA or ACT-D. **(A)** The levels of fibrillarin, UBF1/2, 53BP1, γ H2AX and CARM1 were analysed in promoters of ribosomal genes and rDNA encoding 28S rRNA. Quantification of the studied protein levels by ImageJ software is shown in panel **(B)**. “NC” indicates negative control and “C” indicates non-treated cells. Significantly increased values for EA (ACT-D) from control samples are marked by * (#). Decreased values are pointed out by red signs * (#). Student’s *t*-tests (performed by SigmaPlot software, version 8.0; Jandel Scientific) were used for data evaluation.

ACT-D (Hiscox, 2002; 2007; Calle et al., 2008; Lindenboim et al., 2010). Concerning the histone code, nucleolus is a site of accumulation of histone H1 (Stoldt et al., 2007; Takata et al., 2007) and pronounced nucleolar localization of H1 was prominently observed in G1 phase of the cell cycle (Stoldt et al., 2007). Moreover, it has been reported that proteins of the nucleolus are highly dynamic, for example, nucleolar histone H2B (Musinova et al., 2011) and heterochromatin protein 1 (HP1 β) (Stixová et al., 2011). These experiments showed that the nucleolus, the residence of ribosomal genes, also has its own histone signature (Horáková et al., 2010; Foltánková et al., 2013). Moreover, as shown by ChIP-PCR, ribosomal genes are highly abundant on γ H2AX, even

in non-irradiated genome (Foltánková et al., 2013). Interestingly, ultraviolet (UV) radiation increases γ H2AX significantly and does not induce extensive protein outflow from the nucleolus (Daniely et al., 2002; Foltánková et al., 2013). However, e.g. nucleolin relocates from the nucleolus to the nucleoplasm after cell exposure to ionizing radiation (Daniely et al., 2002). Pronounced reposition was also observed for WRN protein upon oxidative stress (Karmakar and Bohr, 2005), and these experimental conditions also caused relocation of nucleostemin (Huang et al., 2011) or PARP, which moved out of the nucleolus after the cell treatment with an anti-oxidative agent (N-methyl-N’nitro-N-nitrosoguanidine) (Bauer et al., 2001). The pattern of

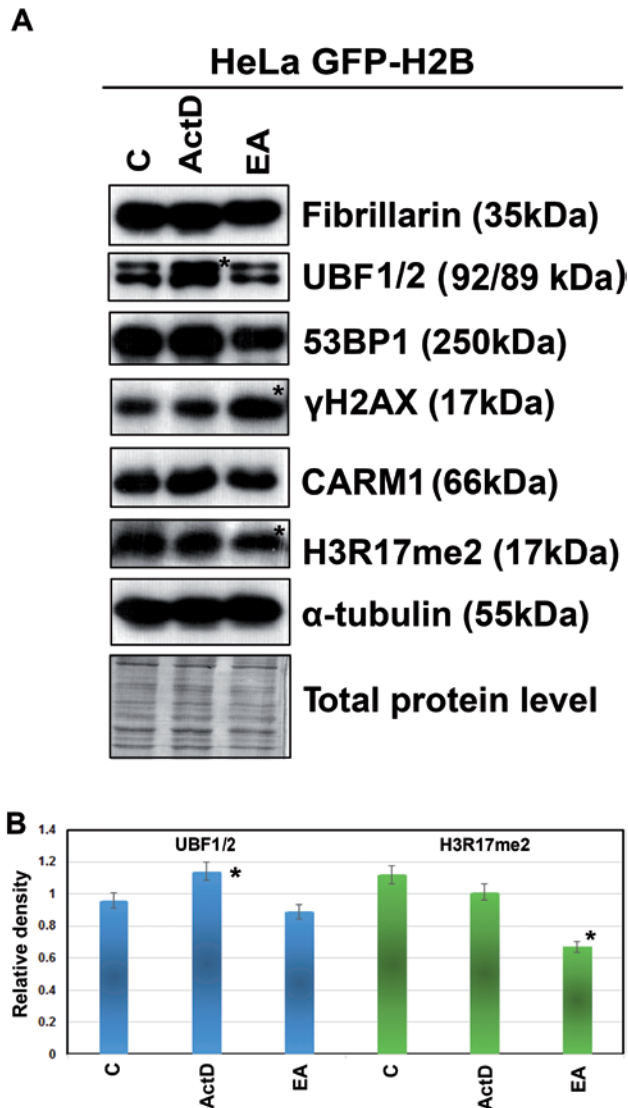


Fig. 7. Protein levels studied by Western blots and protein levels quantified after the treatment of HeLa cells with EA or ACT-D. The following proteins were studied by Western blots **(A)**: fibrillarin, UBF1/2, 53BP1, γ H2AX, CARM1, H3R17me2, and α -tubulin. The protein levels were normalized to total protein levels and α -tubulin levels. Quantification of the density of Western blot fragments **(B)** was performed by NIH ImageJ software for UBF1/2 and H3R17me2.

nucleolar proteins, especially nucleolin, was also changed after coronavirus infection (Dove et al., 2006).

Here, we also showed that ellagic acid is capable of changing the morphology of some proteins of the nucleolus and affects nucleolar protein levels at ribosomal genes. This was compared with ACT-D treatment changing the entire morphology of nucleoli, especially the pattern of fibrillarin, UBF1/2 and RPA194-positive regions (Figs. 3, 4). We showed that EA can change the morphology of only AgNORs and RPA194, but the nuclear patterns of UBF1/2 and fibrillarin were not changed (Figs. 2–4). In addition to its anti-oxidant effect, EA also has an anti-proliferative effect (Fig. 1A), which is especially important in anti-cancer therapy. Intriguingly, the morphological changes induced here by EA were also

accompanied by induction of undesirable 53BP1-positive DNA lesions. The number of 53BP1-positive nuclear bodies was smaller than that observed after ACT-D treatment (Fig. 5D). Based on these results we provided quantification of 53BP1-positive NBs after EA treatment in Fig. 5E. In contrast to our results, Bae et al. (2010) observed that EA has photoprotective effects on collagen breakdown and inflammatory responses in UV-B irradiated human skin cells and hairless mice.

In our studies, the EA and ACT-D effect was additionally associated with cell cycle arrest in G2-M phase of the cell cycle, similarly as strong DNA damage induced by γ -radiation (Fig. 1B; Bártová et al., 2000). Interestingly, Sawicki and Godman (1971) reported that cells are the most sensitive to intoxication with ACT-D in the G1/S interphase or early S phase of the cell cycle. Therefore, this data show that both ACT-D and EA can substantially modify the cell cycle and this effect seems to be cell type-specific, which can also be related to cell cycle progress and RNA half-life in various cell types.

Taken together, we showed that EA has a selective effect on proteins of the nucleolus. Not all proteins of our interest were changed after the EA treatment; only RPA194-positive regions were more condensed. The DNA damaging effect of EA was less pronounced than ACT-D treatment, but the cell numbers were reduced. EA especially affected epigenetic features of the promoters of ribosomal genes. In this genomic region, we found an increased level of fibrillarin, UBF1/2 and γ H2AX, while the levels of 53BP1 and CARM1 were decreased by EA treatment. These data unambiguously pointed EA out as a potential modulator of nucleolar morphology, and EA therefore displays potential to affect processes taking place in this prominent compartment of the cell nucleus.

Acknowledgement

We thank Dr. Pavel Šimara from the Faculty of Informatics, Masaryk University, Brno and Dr. Lenka Stixová from the Institute of Biophysics, Academy of Sciences of the Czech Republic, v. v. i., Brno, Czech Republic for assistance during flow cytometry studies.

References

- Al-Baker, E. A., Oshin, M., Hutchison, C. J., Kill, I. R. (2005) Analysis of UV-induced damage and repair in young and senescent human dermal fibroblasts using the comet assay. *Mech. Ageing Dev.* **126**, 664-672.
- Andersen, J. S., Lam, Y. W., Leung, A. K., Ong, S. E., Lyon, C. E., Lamond, A. I., Mann, M. (2005) Nucleolar proteome dynamics. *Nature* **433**, 77-83.
- Bae, J. Y., Choi, J. S., Kang, S. W., Lee, Y. J., Park, J., Kang, Y. H. (2010) Dietary compound ellagic acid alleviates skin wrinkle and inflammation induced by UV-B irradiation. *Exp. Dermatol.* **19**, e182-190.
- Bártová, E., Kozubek, S., Kozubek, M., Jirsová, P., Lukášová, E., Skalníková, M., Buchníčková, K. (2000) The influence of the cell cycle, differentiation and irradiation on the nu-

- clear location of the *abl*, *bcr* and *c-myc* genes in human leukemic cells. *Leuk. Res.* **24**, 233-241.
- Bauer, P. I., Chen, H. J., Kenesi, E., Kenessey, I., Buki, K. G., Kirsten, E., Hakam, A., Hwang, J. I., Kun, E. (2001) Molecular interactions between poly(ADP-ribose) polymerase (PARP I) and topoisomerase I (Topo I): identification of topology of binding. *FEBS Lett.* **506**, 239-242.
- Boisvert, F. M., van Koningsbruggen, S., Navascues, J., Lamond, A. I. (2007) The multifunctional nucleolus. *Nat. Rev. Mol. Cell Biol.* **8**, 574-585.
- Boulon, S., Westman, B. J., Hutten, S., Boisvert, F. M., Lamond, A. I. (2010) The nucleolus under stress. *Mol. Cell* **40**, 216-227.
- Calle, A., Ugrinova, I., Epstein, A. L., Bouvet, P., Diaz, J. J., Greco, A. (2008) Nucleolin is required for an efficient herpes simplex virus type 1 infection. *J. Virol.* **82**, 4762-4773.
- Castellano, S., Spannhoff, A., Milite, C., Dal Piaz, F., Cheng, D., Tosco, A., Viviano, M., Yamani, A., Cianciulli, A., Sala, M., Cura, V., Cavarelli, J., Novellino, E., Mai, A., Bedford, M. T., Sbardella, G. (2012) Identification of small-molecule enhancers of arginine methylation catalyzed by coactivator-associated arginine methyltransferase 1. *J. Med. Chem.* **55**, 9875-9890.
- Chen, D., Dundr, M., Wang, C., Leung, A., Lamond, A., Misteli, T., Huang, S. (2005) Condensed mitotic chromatin is accessible to transcription factors and chromatin structural proteins. *J. Cell Biol.* **168**, 41-54.
- Daniely, Y., Dimitrova, D. D., Borowiec, J. A. (2002) Stress-dependent nucleolin mobilization mediated by p53-nucleolin complex formation. *Mol. Cell Biol.* **22**, 6014-6022.
- Derenzini, M. (2000) The AgNORs. *Micron* **31**, 117-120.
- Dove, B. K., You, J. H., Reed, M. L., Emmett, S. R., Brooks, G., Hiscox, J. A. (2006) Changes in nucleolar morphology and proteins during infection with the coronavirus infectious bronchitis virus. *Cell. Microbiol.* **8**, 1147-1157.
- Erard, M. S., Belenguer, P., Caizergues-Ferrer, M., Pantaloni, A., Amalric, F. (1988) A major nucleolar protein, nucleolin, induces chromatin decondensation by binding to histone H1. *Eur. J. Biochem.* **175**, 525-530.
- Foltánková, V., Legartová, S., Kozubek, S., Hofer, M., Bártová, E. (2013) DNA-damage response in chromatin of ribosomal genes and the surrounding genome. *Gene* **522**, 156-167.
- Gonzalez-Melendi, P., Wells, B., Beven, A. F., Shaw, P. J. (2001) Single ribosomal transcription units are linear, compacted Christmas trees in plant nucleoli. *Plant J.* **27**, 223-233.
- Govoni, M., Farabegoli, F., Pession, A., Novello, F. (1994) Inhibition of topoisomerase II activity and its effect on nucleolar structure and function. *Exp. Cell Res.* **211**, 36-41.
- Granboulan, N., Granboulan, P. (1965) [Ultrastructure cytochemistry of the nucleolus. II. Study of the sites of RNA synthesis in the nucleolus and the nucleus]. *Exp. Cell Res.* **38**, 604-619.
- Hiscox, J. A. (2002) The nucleolus – a gateway to viral infection? *Arch. Virol.* **147**, 1077-1089.
- Hiscox, J. A. (2007) RNA viruses: hijacking the dynamic nucleolus. *Nat. Rev. Microbiol.* **5**, 119-127.
- Horáková, A. H., Bártová, E., Galiová, G., Uhlířová, R., Matula, P., Kozubek, S. (2010) SUV39h-independent association of HP1 β with fibrillar-ribose-positive nucleolar regions. *Chromosoma* **119**, 227-241.
- Huang, M., Whang, P., Chodaparambil, J. V., Pollyea, D. A., Kusler, B., Xu, L., Felsher, D. W., Mitchell, B. S. (2011) Reactive oxygen species regulate nucleostemin oligomerization and protein degradation. *J. Biol. Chem.* **286**, 11035-11046.
- Karmakar, P., Bohr, V. A. (2005) Cellular dynamics and modulation of WRN protein is DNA damage specific. *Mech. Ageing Dev.* **126**, 1146-1158.
- Kim, J., Lee, J., Yadav, N., Wu, Q., Carter, C., Richard, S., Richie, E., Bedford, M. T. (2004) Loss of CARM1 results in hypomethylation of thymocyte cyclic AMP-regulated phosphoprotein and deregulated early T cell development. *J. Biol. Chem.* **279**, 25339-25344.
- Lam, Y. W., Trinkle-Mulcahy, L., Lamond, A. I. (2005) The nucleolus. *J. Cell Sci.* **118**(Pt 7), 1335-1337.
- Lindenboim, L., Blacher, E., Borner, C., Stein, R. (2010) Regulation of stress-induced nuclear protein redistribution: a new function of Bax and Bak uncoupled from Bcl-x(L). *Cell Death Differ.* **17**, 346-359.
- Moore, H. M., Bai, B., Boisvert, F. M., Latonen, L., Rantanen, V., Simpson, J. C., Pepperkok, R., Lamond, A. I., Laiho, M. (2011) Quantitative proteomics and dynamic imaging of the nucleolus reveal distinct responses to UV and ionizing radiation. *Mol. Cell. Proteomics* **10**, M111.009241.
- Musinova, Y. R., Lisitsyna, O. M., Golyshev, S. A., Tuzhikov, A. I., Polyakov, V. Y., Sheval, E. V. (2011) Nucleolar localization/retention signal is responsible for transient accumulation of histone H2B in the nucleolus through electrostatic interactions. *Biochim. Biophys. Acta* **1813**, 27-38.
- Olson, M. O., Dundr, M. (2005) The moving parts of the nucleolus. *Histochem. Cell Biol.* **123**, 203-216.
- Politz, J. C., Tuft, R. A., Pederson, T. (2003) Diffusion-based transport of nascent ribosomes in the nucleus. *Mol. Biol. Cell* **14**, 4805-4812.
- Raška, I. (2003) Oldies but goldies: searching for Christmas trees within the nucleolar architecture. *Trends Cell Biol.* **13**, 517-525.
- Raška, I., Koberna, K., Malinsky, J., Fidlerova, H., Masata, M. (2004) The nucleolus and transcription of ribosomal genes. *Biol. Cell* **96**, 579-594.
- Raška, I., Shaw, P. J., Cmarko, D. (2006) New insights into nucleolar architecture and activity. *Int. Rev. Cytol.* **255**, 177-235.
- Rohlf, F. J., Sokal, R. R. (1995) *Statistical Tables*. 3rd Edition, W. H. Freeman and Co., New York.
- Sawicki, S. G., Godman, G. C. (1971) On the differential cytotoxicity of actinomycin D. *J. Cell Biol.* **50**, 746-761.
- Scheer, U., Benavente, R. (1990) Functional and dynamic aspects of the mammalian nucleolus. *Bioessays* **12**, 14-21.
- Scherl, A., Coute, Y., Deon, C., Calle, A., Kindbeiter, K., Sanchez, J. C., Greco, A., Hochstrasser, D., Diaz, J. J. (2002) Functional proteomic analysis of human nucleolus. *Mol. Biol. Cell* **13**, 4100-4109.
- Selvi, B. R., Batta, K., Kishore, A. H., Mantelingu, K., Varier, R. A., Balasubramanyam, K., Pradhan, S. K., Dasgupta, D., Sriram, S., Agrawal, S., Kundu, T. K. (2010) Identification of a novel inhibitor of coactivator-associated arginine

- methyltransferase 1 (CARM1)-mediated methylation of histone H3 Arg-17. *J. Biol. Chem.* **285**, 7143-7152.
- Shav-Tal, Y., Blechman, J., Darzacq, X., Montagna, C., Dye, B. T., Patton, J. G., Singer, R. H., Zipori, D. (2005) Dynamic sorting of nuclear components into distinct nucleolar caps during transcriptional inhibition. *Mol. Biol. Cell* **16**, 2395-2413.
- Shaw, P. J., Jordan, E. G. (1995) The nucleolus. *Annu. Rev. Cell Dev. Biol.* **11**, 93-121.
- Stixová, L., Bártová, E., Matula, P., Daněk, O., Legartová, S., Kozubek, S. (2011) Heterogeneity in the kinetics of nuclear proteins and trajectories of substructures associated with heterochromatin. *Epigenetics Chromatin* **4**, 5.
- Stixová, L., Matula, P., Kozubek, S., Gombitová, A., Cmarko, D., Raška, I., Bártová, E. (2012) Trajectories and nuclear arrangement of PML bodies are influenced by A-type lamin deficiency. *Biol. Cell* **104**, 418-432.
- Stoldt, S., Wenzel, D., Schulze, E., Doenecke, D., Happel, N. (2007) G1 phase-dependent nucleolar accumulation of human histone H1x. *Biol. Cell* **99**, 541-552.
- Strašák, L., Bártová, E., Harničarová, A., Galiová, G., Krejčí, J., Kozubek, S. (2009) H3K9 acetylation and radial chromatin positioning. *J. Cell Physiol.* **220**, 91-101.
- Takata, H., Matsunaga, S., Morimoto, A., Ono-Maniwa, R., Uchiyama, S., Fukui, K. (2007) H1.X with different properties from other linker histones is required for mitotic progression. *FEBS Lett.* **581**, 3783-3788.
- Thiry, M., Cheutin, T., O'Donohue, M. F., Kaplan, H., Ploton, D. (2000) Dynamics and three-dimensional localization of ribosomal RNA within the nucleolus. *RNA* **6**, 1750-1761.